2018 IEEE-RAS 18th International Conference on Humanoid Robots (Humanoids)
Beijing, China, November 6-9, 2018

# Mathematical Modeling of Human Body and Movements: On Muscle Fatigue and Recovery based on Energy Supply Systems

Yan Huang[1,2], Yoshihiko Nakamura[1], Yosuke Ikegami[1] and Qiang Huang[2]

*Abstract*— **In this study, we propose a muscle fatigue and recovery model with an energy supply system and physiological basis. Fatigue level is evaluated by maximum muscle contraction force. In the energy supply system, the amounts of aerobic and anaerobic respirations are calculated based on oxygen consumption rate. The variation of related chemical compounds, like lactate and glucose, can be also obtained, which are used to predict the fatigue level. The proposed model is verified by an application to human arm movements. Comparison between the estimated and the measured maximum muscle forces demonstrates the effectiveness of the model.**

## I. Introduction

Mathematical modeling of human body and movements is one of the scientific paradigms that the humanoid robotics develops. Computational algorithms in robotics succeeded to provide the musculoskeletal model of the whole human body (see Fig. 1) [1][2]. Supercomputing has been applied to build and connect the central and peripheral nervous systems and the FEM musculoskeletal system [3]. The scope of this paper is on the inclusion of metabolism into the mathematical models.

Muscle fatigue is a common and complex phenomenon occurring during human exercise, leading to an increased sense of effort. Muscle fatigue is usually defined as a decrease in force generating capacity of a muscle or muscle group after activity [4], which is the collective result of many physiological and neurological processes occurring simultaneously [5]. Since muscle fatigue reduces muscle power and induces discomfort and pain, it is important to predict fatigue and to determine the limits of acceptable muscle loads and exercise intensity [6]. Investigation on muscle fatigue and recovery models can help to explore muscle fatigue mechanism, quantify fatigue level, and guide sport exercise and rehabilitations.

Empirical muscle fatigue models usually focused on describing the relationship between task endurance time and work intensity. For example, K. El ahrache *et al.* employed a statistical analysis of maximum endurance time and percentage of maximum voluntary contraction for the back and upper limbs [7]. However, this kind of model aimed at static tasks and lacked the generality for more complex tasks.

This work was supported by JSPS Grants-in-Aid for Scientific Research (A) JP17H00766, and by the National Natural Science Foundation of China (No. 61603042, 91748202, 61320106012).

[1] Department of Mechanoinformatics, University of Tokyo, 113-8656 Tokyo, Japan.
[2] Beijing Advanced Innovation Center for Intelligent Robots and System, Beijing Institute of Technology, Beijing 100081, China.
E-mail: huang@ynl.t.u-tokyo.ac.jp

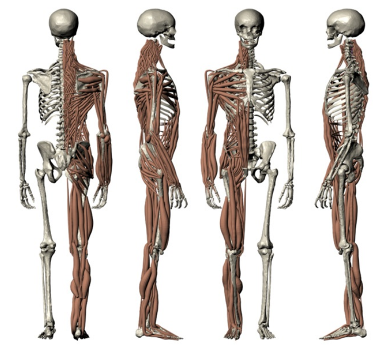

Fig. 1. Musculoskeletal model of the whole human body.

As indicated by [5], theoretical muscle fatigue models often introduce decay terms into existing muscle force models to represent fatigue. Giat *et al.* proposed a mathematical model for the fatigue and recovery phases of a paraplegic's quadriceps muscle subjected to intermittent functional electrical stimulation [8]. Ding *et al.* introduced a four-parameter fatigue model which predicted the fatigue induced by different stimulation patterns on different days during isometric contractions [9]. These approaches were based on detailed muscle activation patterns and muscle contractions were induced by functional electrical stimulations. The models may not be valid to describe voluntary contractions and handle task-related bio-mechanical factors [10].

Another kind of muscle fatigue and recovery model was based on motor units [5][10]. Muscles of these models have three muscle-activation states: resting, activated, and fatigued. Force producing capability of a muscle is proportional to the size of the activated motor unit pool. The model in [10] could accurately predict maximum isometric grip strength and fatigue under the condition in which brain effort is assumed to be constant. However, that approach did not apply to sub-maximal and complex dynamic tasks. Xia and Frey Law proposed a similar three-compartment model which implemented the muscle recruitment hierarchy mathematically and provided an approach to quantitatively evaluate task-related muscle fatigue for complex tasks at the joint level [5].

Most of the existing muscle fatigue and recovery model have not considered the human energy supply system and the physiological process during movements. The interaction between physiological and muscle dynamics was not well studied. In addition, a lot of fatigue models were designed

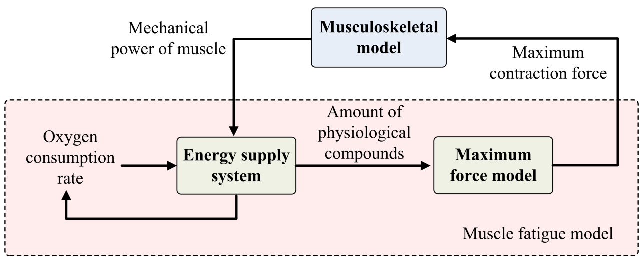


Fig. 2. Flow chart of the proposed model.

for specific movements or isometric tasks, and could not be well generalized to complex motion tasks or dynamic contractions.

In this study, we aim to develop a muscle fatigue and recovery model with considerations of human energy supply systems, including aerobic respiration and anaerobic respiration. The fatigue model describes the relation between mechanical power of muscles and maximum voluntary contraction forces. The proposed model is integrated with a musculoskeletal model, in which an efficient dynamics-computation algorithms for multi-body systems is applied. With this technology, the proposed fatigue model is applicable for multiple muscle cases and complex motion tasks, and may provide insights of interaction between physiological process and muscle dynamics. The proposed model is applied to human arm movements. Parameter identification and fatigue level prediction are realized.

The rest of this paper is as follows. Section II describes the proposed muscle fatigue model and the musculoskeletal model. In Section III, we illustrate the protocol of human motion experiments. Experimental results are shown in Section IV. Section V is discussion and we conclude in Section VI.

## II. Muscle Fatigue Model

Schematic diagram of the proposed model is shown in Fig. 2. Fatigue level is evaluated by the maximum contraction force $F_{max}$. The muscle fatigue model consists of an energy supply system and a maximum force model. The energy supply system simulates the processes of aerobic respirations, anaerobic respirations, and decomposition of adenosine triphosphate ($ATP$) and phosphocreatine ($PCr$). The variations of oxygen consumption rate (OCR) and related physiological compounds can be also obtained. In this study, aerobic respiration refers to complete decomposition of glucose, and anaerobic respiration refers to incomplete decomposition of glucose. Maximum force model is used to estimate $F_{max}$ given the amount of related physiological compounds like lactate and glucose. Muscle force and muscle power can be obtained by inverse dynamics using a musculoskeletal model. Note that $F_{max}$, the output of muscle fatigue model, can also affect the estimation of muscle forces.

### A. Energy supply system

The energy supply system is to simulate the respiration process in human activities. Variations of muscle OCR and the amount of related chemical compounds (e.g. lactate, glucose and phosphoric acid) are calculated based on required muscle power for movements.

In energy supply system, there are three phases: anaerobic respiration-dominant phase, aerobic respiration-dominant phase, and recovery phase (see Fig. 3). The phase judgment is based on comparison between the actual OCR $\dot{V}O_2$ and the desired OCR $\dot{V}O_{2,d}$ obtained from muscle power. When $\dot{V}O_2$ is less than $\dot{V}O_{2,d}$, which often happens in the beginning of movements, anaerobic respiration will be the dominant energy supply mode (see Fig. 3 (a)) and $\dot{V}O_2$ will rise up. $\dot{V}O_2$ is used for aerobic respiration, in which glucose is fully decomposed into carbon dioxide and water and produce energy. However, the energy provided by aerobic respiration can not satisfy the energy consumption of muscles. The insufficient part is firstly provided by $ATP$. If $ATP$ is exhausted, $PCr$ will be decomposed to supply energy. If $PCr$ is also exhausted, glucose starts to be decomposed into lactate to generate energy.

When $\dot{V}O_2$ is equal to $\dot{V}O_{2,d}$, aerobic respiration will be dominant. But there is still a small amount of energy provided by anaerobic respiration. $\dot{V}O_2$ remain constant in this phase.

When $\dot{V}O_2$ is larger than $\dot{V}O_{2,d}$, the muscle will be in recovery phase and the extra oxygen will be consumed by aerobic respiration to produce energy, which is used to supplement $ATP$, $PCr$ and decompose accumulated lactate. $ATP$ supplement and lactate decomposition occur simultaneously at the beginning of recovery phase. When $ATP$ is complemented, $PCr$ supplement starts. In this phase, $\dot{V}O_2$ decreases.

The process of anaerobic respiration can be represented as:

$$ATP \rightarrow ADP + P + 32KJ \quad (1)$$

$$PCr \rightarrow Cr + P + 43KJ \quad (2)$$

$$G \rightarrow 2LA + 2ATP \quad (3)$$

where $ADP$ is adenosine diphosphate, $P$ is phosphoric acid, and $Cr$ is creatine. $G$ and $LA$ represent glucose and lactate, respectively. Note that the formulations in this study are not strict chemical equations. They are just to show the relations among chemical substances. $1mol$ $ATP$ can produce energy of $32KJ$, and $1mol$ $PCr$ can produce energy of $43KJ$. However, not all of these energy can be used for muscle works. A large part of the energy is transformed to heat. In this study, the parameter $R^{M}_{ATP}$ is used to represent the ratios of energy for mechanical work to the total energy produced by $ATP$. In anaerobic respiration, a part of the energy produced by incompletely decomposition of glucose is used to generate $ATP$, then the $ATP$ is decomposed to generate energy for muscles. A parameter $R^{ATP}_{G}$ is used to represent the ratio of energy stored in $ATP$ to the total energy produced by incompletely decomposition of glucose. Thus

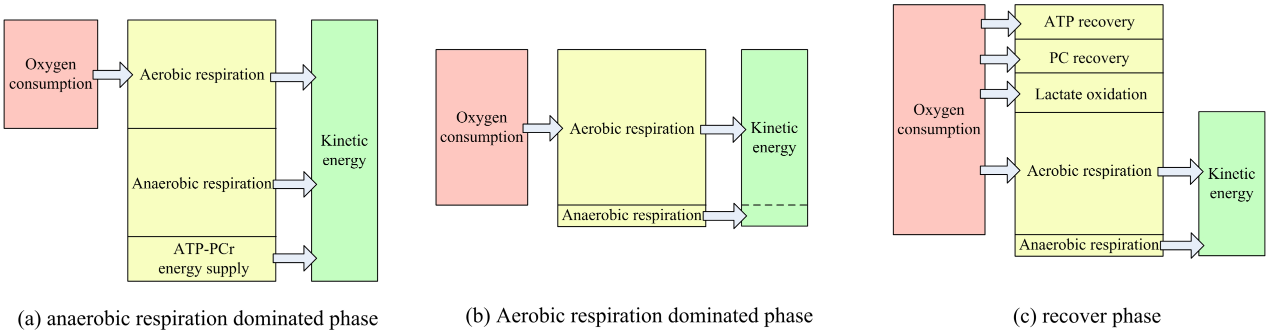


Fig. 3. Three phases of energy supply system: (a) anaerobic respiration-dominant phase; (b) aerobic respiration-dominant phase; and (c) recovery phase.

the incompletely decomposition of $1mol$ glucose can finally produce energy of $R_G^{ATP} R_{ATP}^M$ for muscle mechanical works.

The process of aerobic respiration can be simply represented as:

$$G + 6O_2 \rightarrow 30ATP \tag{4}$$

$O_2$ stands for oxygen. The ratio of energy stored in $ATP$ to the total energy produced by complete decomposition of glucose is denoted as $R_{GO}^{ATP}$.

The process of $ATP$ and $PCr$ regeneration in recovery phase can represented as:

$$ADP + P + 32KJ \quad \rightarrow \quad ATP \tag{5}$$
$$Cr + P + 43KJ \quad \rightarrow \quad PCr \tag{6}$$

The accumulated lactate is decomposed into water and carbon dioxide and produce energy in recovery phase. The process can be represented as:

$$LA + 3O_2 \rightarrow 14ATP \tag{7}$$

The ratio of energy stored in $ATP$ to the total energy produced by decomposition of lactate is denoted as $R_{LA}^{ATP}$. In recovery phase, the ratio of oxygen used for lactate oxidation to the total extra oxygen is denoted as $O_{ex}^{LA}$.

Previous studies showed that the variation of OCR over time during human exercise can be approximated by double exponential functions [11]. In the proposed model, we also employ double exponential functions to characterize the change of $\dot{V}O_2$ of muscles. In anaerobic respiration-dominant phase, the increase of $\dot{V}O_2$ can be mathematically represented as:

$$\dot{V}O_2 = \begin{cases} \dot{V}O_{2,base}, & t \le TD_1 \\ \dot{V}O_{2,base} + A_1(1 - e^{-(t-TD_1)/\tau_1}), & \\ & TD_1 < t < TD_2 \quad or \\ & t > TD_1, \dot{V}O_{2\_des} \le \dot{V}O_{2,LA} \\ \dot{V}O_{2,base} + A_1(1 - e^{-(t-TD_1)/\tau_1}) & \\ +A_2(1 - e^{-(t-TD_2)/\tau_2}), & \\ & t > TD_2,\ \dot{V}O_{2\_des} > \dot{V}O_{2,LA} \end{cases} \tag{8}$$

where $t$ represents time, $\dot{V}O_{2,base}$ is the oxygen consumption rate at rest or at the previous stable state. $\dot{V}O_{2,LA}$ indicates the oxygen consumption rate at lactate threshold. When $\dot{V}O_2$ exceeds $\dot{V}O_{2,LA}$, the rising speed decreases, anaerobic respiration is enhanced and lactate increases. The second exponential term in equation 8 appears only when oxygen consumption rate is larger than $\dot{V}O_{2,LA}$. $\tau_1$ and $\tau_2$ are the time constants of the two exponential curves, respectively. $TD_1$ represent the circulatory transit delay between muscles and lungs, and $TD_2$ indicates the time instant when oxygen consumption rate reaches to $\dot{V}O_{2,LA}$. $A_1$ and $A_2$ are the amplitudes of the two exponential processes, respectively. We denote the upper limit of $\dot{V}O_2$ as $\dot{V}O_{2,max}$. If $\dot{V}O_{2,des}$ is less than $\dot{V}_{O2,max}$, $A_1 + A_2$ equals to $\dot{V}O_{2\_des} - \dot{V}O_{2,base}$, otherwise $A_1 + A_2$ equals to $\dot{V}_{O2,max} - \dot{V}O_{2,base}$. $A_1$ is usually equal to $\dot{V}O_{2,LA} - \dot{V}O_{2,base}$.

In recovery phase, the decrease of $\dot{V}O_2$ can be mathematically represented as:

$$\dot{V}O_2 = \begin{cases} \dot{V}O_{2,base}, & t \le TD_3 \\ \dot{V}O_{2,base} - A_3(1 - e^{-(t-TD_3)/\tau_3}), & \\ & TD_3 < t < TD_4 \\ \dot{V}O_{2,base} - A_3(1 - e^{-(t-TD_3)/\tau_3}) & \\ -A_4(1 - e^{-(t-TD_4)/\tau_4}), & \\ & t > TD_4 \end{cases} \tag{9}$$

where $\tau_3$ and $\tau_4$ are time constants of the primary and slow exponential terms, respectively. $TD_3$ and $TD_4$ are time delays of these two terms. $A_3 + A_4$ equals $\dot{V}O_{2,base} - \dot{V}O_{2\_des}$.

## B. Maximum force model

The maximum force model describes the effects of physiological variables on maximum contraction force, which indicates the fatigue level.

Muscle fatigue is a complex phenomenon, and the cause of fatigue includes many factors. The three main causes are depletion of muscle glucose, accumulation of lactate, and the increase of phosphoric acid [4], which can decrease muscle PH, interfere the combination of Calcium ion and troponin, and reduce muscle contraction ability. In the proposed model, three linear functions are used to represent the relations between these three factors and muscle behaviors:

$$F_{LA} = \begin{cases} 1, & LA \leq LA_t \\ 1 - \frac{(1-F_{LA,min})(LA-LA_t)}{LA_{max}-LA_t}, & LA > LA_t \end{cases} \tag{10}$$

$$F_P = \begin{cases} 1, & P \leq P_t \\ 1 - \frac{(1-F_{P,min})(P-P_t)}{P_{max}-P_t}, & P > P_t \end{cases} \tag{11}$$

$$F_G = \begin{cases} 1, & G \geq G_t \\ 1 - \frac{(1-F_{G,min})(G_t-G)}{G_t-G_{min}}, & G < G_t \end{cases} \tag{12}$$

$F_{LA}$, $F_P$, $F_G$ are the reduction factors of the maximal muscle force $F_{max}$. $F_{LA,min}$, $F_{P,min}$ and $F_{G,min}$ are the lower limits of these reduction factors. $LA_t$, $P_t$ and $G_t$ are the threshold values of lactate, phosphoric acid and glucose, respectively, which trigger decline of $F_{max}$. $LA_{max}$, $P_{max}$, and $G_{min}$ are the maximum amount of lactate, the maximum amount of phosphoric acid and the minimum amount of glucose in the muscle, respectively. The current $F_{max}$ equals $F_{LA} \cdot F_P \cdot F_G \cdot F_{max\_o}$. $F_{max\_o}$ is the value of $F_{max}$ at rest.

## III. Human Motion Experiments

To verify the feasibility of the proposed model, we applied the proposed approach to the analysis of human arm movements. Fatigue of biceps and triceps was studied. The experimental scene is shown in Fig. 4 and the experimental procedure is shown in Fig. 5.

Three male subjects (subject 1: 23 years old, 172$cm$ height, 58$kg$ weight; subject 2: 23 years old, 168$cm$ height, 60$kg$ weight; subject 3: 23 years old, 172$cm$ height, 68$kg$ weight) were recruited in the experiment. All subjects provided informed consent prior to the participation. Each trial had a time duration of 1 minute, including arm movement and maximum force measurement. In the first 45 seconds, each subject was asked to repeatedly bend and stretch the right elbow joint with a 1.5$kg$ stick in the hand. The upper arm kept upright and the lower arm moved between 90 degrees of flexion and upright posture, following an indicator in a video in front of the subject. In the rest 15 seconds, the subject put down the stick and tried his best to pull up and pull down two cables connected to two force sensors (IMADA, Japan) in turn. The two force sensors were fixed on a structure connected to the ground. After about 10 trials, when the subject had an obvious sense of fatigue, the movements were stopped and the subject started to rest, but the maximum force was still measured once a minute. When the subject felt completely recovered from fatigue, the experiment was stopped. Each subject performed experiments with three arm rotation frequencies: 0.18$Hz$, 0.30$Hz$, 0.48$Hz$. The frequency was adjusted by changing the speed of the indicator in the video. Each experiment was at least two days apart.

During arm movements, human motion data was measured by an optical motion capture system (Motion Analysis Corporation, Santa Rosa, CA, USA) with 12 cameras at 200$Hz$ and 6 markers (one at shoulder, two at elbow joint, two at wrist joint and one at hand). Electromyogram (EMG) signals were measured by a wireless electromyograph system (Nihon Kohden, Tokyo, Japan) with 5 channels (two at biceps and three at triceps) at 200$Hz$. Muscle forces were obtained by inverse dynamics using a custom-built software which employ robotics algorithms, sDIMS [12]. Then the muscle power can be calculated and used as input of the muscle fatigue model, and $F_{max}$ can be estimated.

Fig. 4. The experimental scene of arm movements.

The musculoskeletal model includes the skeletons of shoulder, upper arm, forearm and hand, and the muscles of biceps brachii and triceps brachii. Note that brachialis, brachioradialis and anconeus are not considered in this model and the elbow torque is generated by only biceps and triceps, thus the maximum forces of biceps and triceps estimated by the proposed model may be larger than the data obtained from biological studies.

The measured maximum force was calculated by the following equations:

$$\begin{aligned} F_T \cdot d_T &= T_s - T_g \\ F_B \cdot d_B &= T_s + T_g \end{aligned} \tag{13}$$

where $F_T$ and $F_B$ are the maximum force of triceps and biceps, respectively. $d_T$ and $d_B$ are the moment arms of biceps force and triceps force around elbow joint, respectively. $T_s$ is the torque of the force pulling up or down the sensor around elbow joint. $T_g$ is the torque of the gravity of forearm around elbow joint. The curves of measured $F_{max}$ were obtained by an exponential fitting method based on the discrete measured maximum force data at the end of each trial.

In this study, the parameters of muscle fatigue model were identified by an optimization method which minimizes the difference between measured and estimated $F_{max}$. The mathematical representation is:

$$\min_p \int_{t=0}^{t=t_e} \sum_{i=1}^{n} |F_{max}^{e,i} - F_{max}^{m,i}| dt \tag{14}$$

subject to:

$$p_l \leq p \leq p_u \tag{15}$$

where $p$ is the parameter set for optimization, including $\dot{V}_{O2,max}$, $\tau_1$, $\tau_2$, $\tau_3$, $\tau_4$, $F_{LA,min}$, $LA_t$, $F_{P,min}$, $P_t$, $F_{G,min}$ and $G_t$ of biceps and triceps. $i$ is the experiment index, which is from 1 to 3 in this study since we carried out experiments with three rotation speeds. $n$ is the number of experiment. $F_{max}^{e,i}$ is

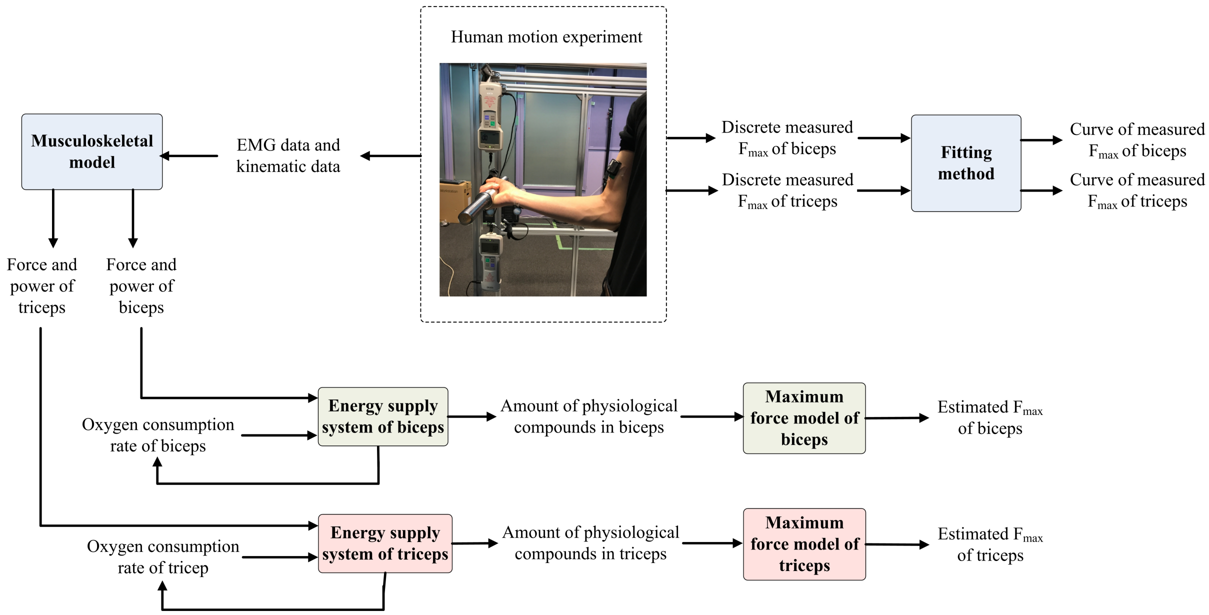


Fig. 5. Schematic diagram of human arm movements and data processing.

the maximum force of experiment $i$ estimated by the model, $F_{max}^{m,i}$ is the maximum force of experiment $i$ obtained by the measured force. The movement starts at $t = 0$ and $t_e$ is the time of fully recovery from fatigue. $p_l$ and $p_u$ are the lower bound and upper bound of $p$, respectively. The optimization was realized by a trust-region-reflective algorithm.

## IV. Results

The parameters of the proposed muscle fatigue model includes general parameters and individual parameters. The values of general parameters are the same for all the subjects and are determined by literature (see Table I). The individual parameters characterize movement ability and fatigue behavior of each subject. The values of individual parameters are subject-specific and task-specific, and are identified by Equation 14.

In this study, the individual parameters of middle speed movement of each subject were identified with the respective measured maximum force used in the cost function. In addition, we also used the measured maximum forces of high speed and low speed movements of subject 1 in the cost function to obtain the individual parameters, and applied this parameter set to the middle speed movement of subject 1, to verify the ability of the proposed model to predict fatigue level of a new movement by collected data. The values of these four individual parameter sets are shown in Table II. $PCr_{rest}$ in Table II is the amount of $PCr$ in muscle at rest.

With the general parameter values and each set of individual parameter values, we calculate the maximum forces of biceps and triceps by the proposed muscle fatigue model. The estimated and measured maximum muscle forces of middle speed movement of each subject are shown in Fig. 6. The estimated maximum force is close to the measured maximum force for each subject. The estimated curves show oscillatory behaviors because the muscle power was set to zero during each maximum force measurement period.

The identified individual parameters show that accumulated lactate is the dominate factor of muscle fatigue in this motion task. Subject 1 and subject 3 have relatively high OCR, which indicates their strong aerobic respiration ability. Subject 2 has a higher fatigue threshold value of lactate $LA_t$, thus the decrease of maximum muscle force of subject 2 appeared later than those of the other two subjects. $F_{LA,min}$ of subject 2 is also the largest, thus the decline of maximum force of subject 2 is the smallest.

Fig. 7 shows the results of applying individual parameters obtained by high and low speed movements to middle speed movement of subject 1. Although the parameters were identified by movements of other intensities, the estimated maximum force could still well predict the variation of measured maximum force, which indicates that the obtained individual parameters for a specific subject is applicable to different motion intensities. Similar results are also obtained for subject 2 and subject 3. The variation of OCR and chemical compounds showed similar trends with those reported by literature [13]. The results indicated that the OCR and energy consumption of triceps were lower than those of biceps in the studied arm movement.

## V. Discussion

Human energy supply system is combined with muscle fatigue behavior in the proposed model. By using this model, we can predict muscle fatigue level during movement and recovery phases, and also explore the underlying causes of muscle fatigue. The muscle fatigue model is applied to a musculoskeletal model. The mechanical power of muscle is

TABLE I

VALUES OF GENERAL PARAMETERS.

| Parameter | Description | Value of biceps | Value of triceps |
|---|---|---|---|
| $ATP_{rest}$ | the amount of ATP at rest | 21 $mmol$ | 7.0 $mmol$ |
| $ATP_{min}$ | the minimum amount of ATP | 0 $mmol$ | 0 $mmol$ |
| $PCr_{min}$ | the minimum amount of PCr | 0 $mmol$ | 0 $mmol$ |
| $LA_{rest}$ | the amount of lactate at rest | 2.0 $mmol$ | 2.0 $mmol$ |
| $LA_{max}$ | the maximum amount of Lactate | 22 $mmol$ | 22 $mmol$ |
| $G_{rest}$ | the amount of glycose at rest | 55 $mmol$ | 55 $mmol$ |
| $G_{min}$ | the minimal amount of glycose | 0 $mmol$ | 0 $mmol$ |
| $TD_1$ | time constant of OCR curve | 8.0$s$ | 8.0$s$ |
| $TD_3$ | time constant of OCR curve | 10$s$ | 10$s$ |
| $TD_4$ | time constant of OCR curve | 11$s$ | 11$s$ |
| $G_{min}$ | the minimal amount of glycose | 0 $mmol$ | 0 $mmol$ |
| $R_{ATP}^{M}$ | energy ratio parameter | 0.30 | 0.30 |
| $R_{GO}^{ATP}$ | energy ratio parameter | 0.40 | 0.40 |
| $R_{G}^{ATP}$ | energy ratio parameter | 0.40 | 0.40 |
| $R_{LA}^{ATP}$ | energy ratio parameter | 0.40 | 0.40 |
| $O_{ex}^{LA}$ | ratio of oxygen for lactate oxidation to total extra oxygen in recovery phase | 0.65 | 0.65 |

TABLE II

VALUES OF IDENTIFIED INDIVIDUAL PARAMETERS.

| | Middle speed, Subject 1 | Middle speed, Subject 2 | Middle speed, Subject 3 | High and low speeds, Subject 1 |
|---|---|---|---|---|
| Biceps | | | | |
| $\dot{V}O_{2,max}$ | 1.460 $mmol/s$ | 1.170 $mmol/s$ | 1.490 $mmol/s$ | 1.420 $mmol/s$ |
| $\dot{V}O_{2,LA}$ | 0.8121 $mmol/s$ | 0.6423 $mmol/s$ | 0.9843 $mmol/s$ | 0.8593 $mmol/s$ |
| $\tau_1$ | 26.26 $s$ | 15.20 $s$ | 18.38 $s$ | 18.59 $s$ |
| $\tau_2$ | 62.37 $s$ | 60.25 $s$ | 68.29 $s$ | 61.63 $s$ |
| $\tau_3$ | 457.8 $s$ | 300.2 $s$ | 523.4 $s$ | 499.0 $s$ |
| $\tau_4$ | 1012 $s$ | 1003 $s$ | 923.4 $s$ | 1011 $s$ |
| $PCr_{rest}$ | 77.20 $mmol$ | 79.34 $mmol$ | 72.72 $mmol$ | 75.20 $mmol$ |
| $F_{LA,min}$ | 0.7830 | 0.9134 | 0.7232 | 0.8038 |
| $LA_t$ | 3.470 $mmol$ | 5.340 $mmol$ | 4.230 $mmol$ | 3.610 $mmol$ |
| $F_{G,min}$ | 0.9654 | 0.9648 | 0.9739 | 0.9674 |
| $G_t$ | 50.65 $mmol$ | 50.76 $mmol$ | 52.38 $mmol$ | 48.99 $mmol$ |
| $F_{P,min}$ | 0.9539 | 0.9894 | 0.9483 | 0.9294 |
| $P_t$ | 48.28 $mmol$ | 50.22 $mmol$ | 56.21 $mmol$ | 41.21 $mmol$ |
| Triceps | | | | |
| $\dot{V}O_{2,max}$ | 0.2183 $mmol$ | 0.4185 $mmol/s$ | 0.4983 $mmol/s$ | 0.1738 $mmol/s$ |
| $\dot{V}O_{2,LA}$ | 0.1649 $mmol$ | 0.3373 $mmol/s$ | 0.3898 $mmol/s$ | 0.1352 $mmol/s$ |
| $\tau_1$ | 36.62 $s$ | 47.97 $s$ | 56.73 $s$ | 38.11 $s$ |
| $\tau_2$ | 56.38 $s$ | 61.43 $s$ | 64.19 $s$ | 55.21 $s$ |
| $\tau_3$ | 542.4 $s$ | 379.2 $s$ | 307.5 $s$ | 536.4 $s$ |
| $\tau_4$ | 1535 $s$ | 1616 $s$ | 1382 $s$ | 1506 $s$ |
| $PCr_{rest}$ | 29.18 $mmol$ | 26.97 $mmol$ | 28.28 $mmol$ | 27.29 $mmol$ |
| $F_{LA,min}$ | 0.7419 | 0.7949 | 0.6093 | 0.7602 |
| $LA_t$ | 3.304 $mmol$ | 4.964 $mmol$ | 4.877 $mmol$ | 3.021 $mmol$ |
| $F_{G,min}$ | 0.9683 | 0.9764 | 0.9423 | 0.9668 |
| $G_t$ | 51.39 $mmol$ | 52.33 $mmol$ | 49.32 $mmol$ | 52.51 $mmol$ |
| $F_{P,min}$ | 0.9529 | 0.9220 | 0.9638 | 0.9339 |
| $P_t$ | 18.02 $mmol$ | 15.53 $mmol$ | 11.86 $mmol$ | 22.36 $mmol$ |

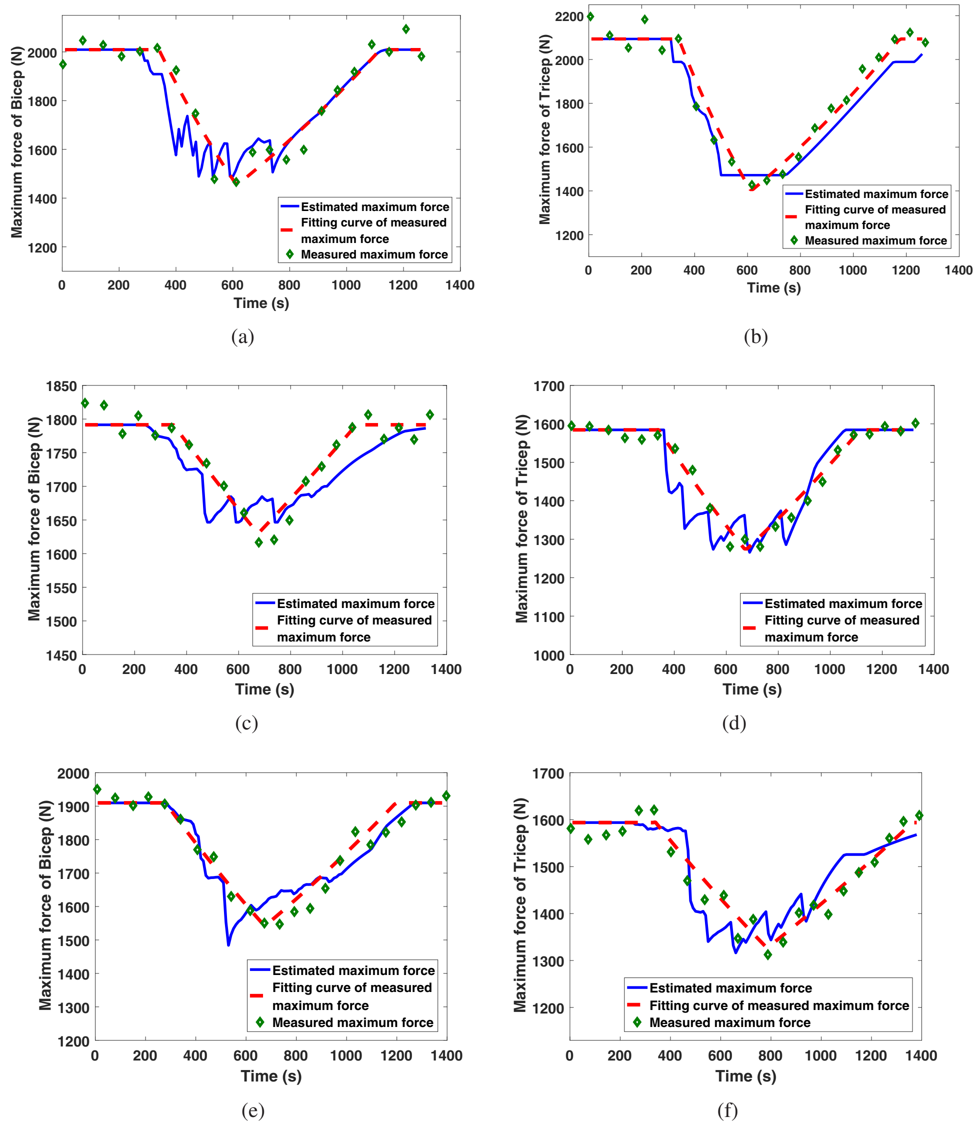


Fig. 6. The maximum forces of middle speed movements of the three subjects. (a): maximum force of biceps of subject 1; (b): maximum force of triceps of subject 1; (c): maximum force of biceps of subject 2; (d): maximum force of triceps of subject 2; (e): maximum force of biceps of subject 3; (f): maximum force of triceps of subject 3.

the input of the fatigue model and the fatigue model outputs maximum muscle forces to the musculoskeletal model, which makes a closed loop of muscle dynamics, mechanical energy and physiological processes. This is the novelty of the proposed model.

There are also some limitations of this study. The model has a lot of parameters to be identified, which results in a heavy calculation load, especially when the muscle number is large. Development of an efficient algorithm is an important future work.

## VI. Conclusion

In this study, a muscle fatigue and recovery model with energy supply system and physiological basis is proposed. Maximum muscle force can be calculated to evaluated fatigue level. The oxygen consumption rate and chemical compounds can be also obtained, which may provide further insights of muscle fatigue. The model was applied to human arm movement. Motion data were collected during human motion experiments. Comparison between estimated and measured maximum muscle forces showed that the model could well predict muscle fatigue level.

There are several ways to extend this study. Developing an efficient algorithm for parameter identification could be helpful for study of motion tasks involving more muscles. Collecting more data, e.g. oxygen consumption and blood lactate concentration, during human motion experiments can also improve the model.

## References

[1] K. Yamane, Y. Fujita, Y. Nakamura, "Estimation of physically and physiologically valid somatosensory information," *Proc. of IEEE In-*

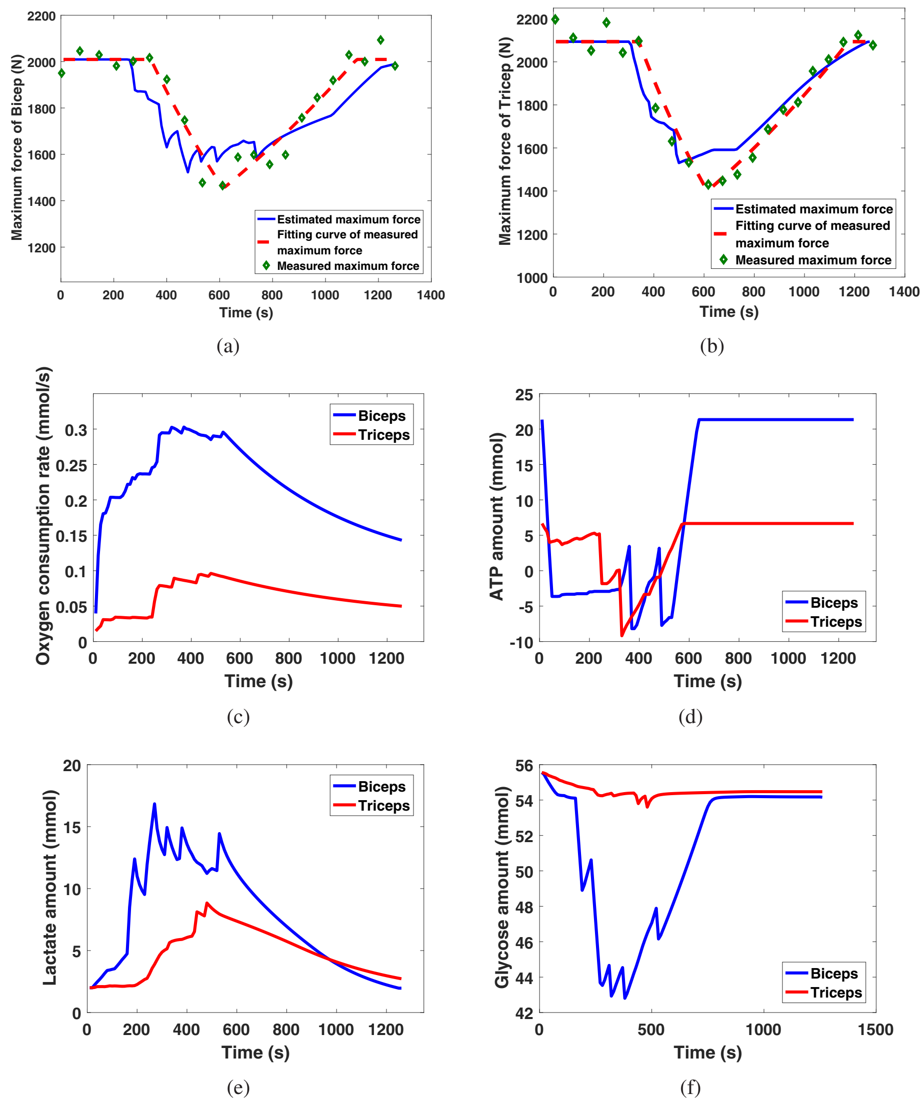


Fig. 7. Maximum force and chemical compound amounts of biceps and triceps of middle speed movement of subject 1. (a): maximum force of biceps; (b): maximum force of triceps; (c): Oxygen consumption rate of biceps and triceps; (d): ATP of biceps and triceps; (e): lactate of biceps and triceps; (f): glucose of biceps and triceps.


*ternational Conference on Robotics and Automation*, pp. 2635-2641, Barcelona, Spain, 2005.

[2] K. Ayusawa, Y. Nakamura, "Fast inverse kinematics algorithm for large dof system with decomposed gradient computation based on recursive formulation of equilibrium, *IEEE/RSJ International Conference on Intelligent Robots and Systems*, pp. 3447-3452, Vilamoura, Portugal, 2012.

[3] K. Hirasawa, K. Ayusawa, Y. Nakamura, "Muscle activity estimation based on inverse dynamics and muscle stress analysis by finite element method." *CISM-IFToMM Symposium on Robot Design, Dynamics, and Control*, ID-45, Paris, France, 2012.

[4] B. Bigland-Ritchie, J. J. Woods, "Changes in muscle contractile properties and neural control during human muscular fatigue," *Muscle Nerve*, vol. 7, pp. 691-699, 1984.

[5] T. Xia, L. A. Frey Law, "A theoretical approach for modeling peripheral muscle fatigue and recovery," *J. of Biomech.*, vol. 41, pp. 3046-3052, 2008.

[6] L. Ma, D. Chablat, F. Bennis, W. Zhang, "A new simple dynamic muscle fatigue model and its validation," *Int. J. Ind. Ergon.*, vol, 39, pp. 211-220, 2009

[7] K. El ahrache, D. Imbeau, B. Farbos, "Percentile values for determining maximum endurance times for static muscular work." *Int. J. Ind. Ergon.*, vol. 36, pp. 99-108, 2006.

[8] Y. Giat, J. Mizrahi, M. Levy, "A model of fatigue and recovery in paraplegics quadriceps muscle subjected to intermittent FES," *J. Biomech. Eng.-Trans. ASME*, vol. 118, pp. 357-366, 1996.

[9] J. Ding, A. S. Wexler, S. A. Binder-Macleod, "A predictive model of fatigue in human skeletal muscles," *J. Appl. Physiol.*, vol. 89, pp. 1322-1332, 2000.

[10] J. Z. Liu, R. W. Brown, G. H. Yue, "A dynamical model of muscle activation, fatigue, and recovery," *Biophys. J.*, vol. 82, pp. 2344-2359, 2002.

[11] T. J. Barstow, P. A. Mole, "Linear and nonlinear characteristics of oxygen consumption kinetics during heavy exercise," *J. Appl. Physiol.*, vol. 71, pp. 2099-2106, 1991.

[12] Y. Nakamura, K. Yamane, Y. Fujita, I. Suzuki, "Somatosensory computation for man-machine interface from motion-capture data and musculoskeletal human model," *IEEE Tran. Robot.*, vol. 21, no. 1, 2005.

[13] W. L. Roston, B. J. Whipp, J. A. Davis, D. A. Cunningham, R. M. Effros, K. Wasserman, "Oxygen uptake kinetics and lactate concentration during exercise in humans," *Am. Rev. Respir. Dis.*, vol. 135, no. 5, pp. 1080-1084, 1987.